Characteristics of light polarization in magneto-optic fiber Bragg gratings with linear birefringence

Baojian Wu (武保剑)*, Chongzhen Li (李崇真), Kun Qiu (邱 昆), and Liwei Cheng (程立伟)

Key Lab of Broadband Optical Fiber Transmission and Communication Networks of the Ministry of Education, University of Electronic Science and Technology of China, Chengdu 610054, China

**Corresponding author: bjwu@uestc.edu.cn*

Received June 22, 2010; accepted August 11, 2010; posted online January 1, 2011

The coupling between guided optical waves in magneto-optic fiber Bragg gratings (MFBGs) with linear birefringence is investigated using the eigen-mode and coupled-mode approaches. The relationship between the polarization-dependent loss (PDL) and the eigen states of polarization (SOPs) in the MFBGs is discussed. Only the MFBGs with low linear birefringence are applied to the peak PDL-based magnetic field measurement, after which the linear dynamic range is determined using the relative magnitude of linear and magnetically induced circular birefringence. In this letter, a theoretical model is presented to explain the experimental results and help develop novel MFBG-based devices.

OCIS codes: 060.3735, 230.2240, 060.2300.

doi: 10.3788/COL201109.010601.

With the extensive applications of fiber Bragg gratings (FBGs) in optical communication systems[1] and optical sensors, composite or rare-earth-doped special FBGs have also attracted attention for use in optical signal processing[2,3]. Magneto-optic FBGs (MFBGs) comprise a class of special FBGs associated with the magneto-optical (MO) effects, such as the Faraday effect. In principle, the rare-earth-doped FBGs or writing FBGs on strain-tuned yttrium-iron-garnet (YIG) fibers[4] should be used for large MO coefficients similar to those in the mechanically microfabricated YIG planar gratings[5]. The MFBGs are promising candidates for current or magnetic field sensors and tunable dispersion compensation modules[6]. Kersey *et al.* described a novel fiber probe for monitoring alternating current (AC) high magnetic fields by detecting the shift in Bragg condition of FBGs due to magnetically induced circular birefringence[7]. Arce-Diego *et al.* compared the shift values for silica and terbium-doped optical fibers[8]. The magnetic tunability of the MFBGs is expected to have a unique advantage over the often-used tuning schemes in compensating or tracking speed due to the immediate magnetic field response of the MFBGs, which is free of any extra stretcher (e.g., magnetostrictive rod).

In practice, the conventional FBGs used in optical communications and fiber sensing may also be regarded as MFBGs, to a certain extent, if the weak MO effects in fibers are taken into account. However, a small linear birefringence in standard fibers can lead to the quenching of the Faraday effect[9]. Thus, to utilize the intrinsic MO effects in the silica FBGs at the present time, one has to recur to high-resolution detection technologies, such as unbalanced Mach-Zehnder interferometers[9] and polarization-dependent loss (PDL)[10,11]. However, it should also be pointed out that the coupling of guided optical waves (GOWs) in the MFBGs tends to be more complicated than the case in the magneto-optic fibers because of the grating reflection. To our knowledge, thorough investigations have not yet been conducted on the influence of linear birefringence on the propagation characteristics of guided light in the MFBGs until now. In this letter, we propose a theoretical model of MFBGs, which includes linear birefringence, MO effect (or magnetically-induced circular birefringence), and grating Bragg diffraction. In the MFBGs, the analytic expression of the eigen states of polarization (SOPs) can be derived using the eigen-mode approach, in which the above-mentioned effects are introduced one by one as perturbations into the MFBG systems. These effects, as a whole, may also be taken into account through the coupled-mode approach.

In linear birefringent MFBGs, the MO coupling of two orthogonal linear polarization modes depends on the phase mismatch resulting from linear birefringence just as in MO film waveguides[12]. The Bragg grating structure is responsible for the coupling between the incident and reflected light beams. In the following, the Faraday MO effect and refractive index modulation of FBGs are added in succession into a linear birefringent fiber system; a lightwave coupling problem in the linear birefringent MFBGs is partitioned into two sub-problems of x-invariant MO waveguides and MO waveguide gratings.

The first sub-problem is necessary for the perturbation method to obtain the total optical field in the MFBGs of interest. Provided that the GOWs are confined to the fiber core for fundamental modes, the optical field $\mathbf{E}(x,y,z,t)$ associated with the MO perturbation can be restructured from the eigen modes by

$$\mathbf{E}(x,y,z,t)=\frac{1}{2}\mathbf{F}(y,z)\big[\hat{y}A_y(x)\mathrm{e}^{\mathrm{j}(\omega t-\beta_y x)}+\hat{z}A_z(x)\mathrm{e}^{\mathrm{j}(\omega t-\beta_z x)}\big]+c.c. \quad , \quad (1)$$

where the fast and slow axes of linearly birefringent fibers are taken as the y and z axes, respectively; $\mathbf{F}(y,z)$ is the normalized transversal distribution of the electric field; $A_y(x)$ and $A_z(x)$ are the complex amplitudes; *c.c.* designates the complex conjugate of the former terms; $\beta_y=n_{\mathrm{f}}k_0$ and $\beta_z=n_{\mathrm{s}}k_0$ are the propagation constants of the y- and z-polarized GOWs at the angular frequency ω, respectively (where, n_{s} and n_{f} are the refractive in-

dices along the slow and fast axes, respectively); $k_0 = \omega/c$ (where c is the light speed in vacuum).

Similar to the MO film waveguides, substituting Eq. (1) into the coupled-mode equations in the presence of the MO perturbation[13] results in:

$$\begin{cases} \dfrac{\mathrm{d}A_z(x)}{\mathrm{d}x} = -\kappa_{\mathrm{m}} \mathrm{e}^{\mathrm{j}\Delta\beta x} A_y(x) \\ \dfrac{\mathrm{d}A_y(x)}{\mathrm{d}x} = \kappa_{\mathrm{m}} \mathrm{e}^{-\mathrm{j}\Delta\beta x} A_z(x) \end{cases}, \tag{2}$$

where $\Delta\beta = \beta_z - \beta_y = (n_{\mathrm{s}} - n_{\mathrm{f}})\, k_0$, and $\kappa_{\mathrm{m}} = \frac{k_0 f_1 M_{0x}}{2n_0} = k_0 \Delta n_{\mathrm{m}}$ is the MO coupling coefficient, in which f_1 and M_{0x} are the Faraday factor and static magnetization along the x direction, respectively. In addition, $n_0 = \frac{1}{2}(n_{\mathrm{s}} + n_{\mathrm{f}})$ is the average refractive index of the medium, and $\Delta n_m = \frac{f_1 M_{0x}}{2n_0}$ is the refractive index variation induced by the Faraday effect. From the viewpoint of the Faraday rotation, it can be proven easily that $\kappa_{\mathrm{m}} = V_{\mathrm{B}}\mathbf{B} = \phi_{\mathrm{F}}$, where V_{B} and $\mathbf{B}$ are the Verdet constant and the applied magnetic field, respectively, and ϕ_{F} is the specific Faraday rotation. The solution of Eq. (2) can be expressed by

$$\mathbf{B}(x) = \mathbf{M}(x) \cdot \mathbf{B}(0), \tag{3}$$

where $\mathbf{B}(x) = \begin{bmatrix} A_y(x)\mathrm{e}^{\mathrm{j}\frac{\Delta\beta}{2}x} \\ A_z(x)\mathrm{e}^{-\mathrm{j}\frac{\Delta\beta}{2}x} \end{bmatrix}$ and $\mathbf{M}(x) = \begin{bmatrix} \cos\kappa x + \mathrm{j}\cos\tau\sin\kappa x & \sin\tau\sin\kappa x \\ -\sin\tau\sin\kappa x & \cos\kappa x - \mathrm{j}\cos\tau\sin\kappa x \end{bmatrix}$, in which $\sin\tau = \frac{\kappa_{\mathrm{m}}}{\kappa}$ and $\cos\tau = \frac{\Delta\beta}{2\kappa} = \frac{\kappa_{\mathrm{b}}}{\kappa}$, $\kappa = \sqrt{\left(\frac{\Delta\beta}{2}\right)^2 + |\kappa_{\mathrm{m}}|^2} = \sqrt{\kappa_{\mathrm{b}}^2 + \kappa_{\mathrm{m}}^2}$, $\kappa_{\mathrm{b}} = \frac{\Delta\beta}{2} = \frac{1}{2}(n_{\mathrm{s}} - n_{\mathrm{f}})\, k_0 = k_0 \Delta n_{\mathrm{b}}$, and $\Delta n_{\mathrm{b}} = \frac{1}{2}(n_{\mathrm{s}} - n_{\mathrm{f}})$ is the refractive index change resulting from the linear birefringence. Utilizing the transform of unit basis vectors $\hat{\mathbf{e}}_+ = \frac{\hat{y} + \mathrm{j}\eta\hat{z}}{\sqrt{1+\eta^2}}$ and $\hat{\mathbf{e}}_- = \frac{\eta\hat{y} - \mathrm{j}\hat{z}}{\sqrt{1+\eta^2}}$ with the ellipticity $\eta = \tan\frac{\tau}{2}$, one can obtain the corresponding elliptically polarized components expressed by

$$\begin{aligned} \mathbf{E}_{0+}(x) &= \cos(\tau/2)\left[A_y(0) - \mathrm{j}\eta A_z(0)\right]\exp(\mathrm{j}\kappa x) \\ &= \mathbf{E}_{0+}(0)\exp(\mathrm{j}\kappa x) \\ \mathbf{E}_{0-}(x) &= \cos(\tau/2)\left[\eta A_y(0) + \mathrm{j}A_z(0)\right]\exp(-\mathrm{j}\kappa x) \\ &= \mathbf{E}_{0-}(0)\exp(-\mathrm{j}\kappa x) \end{aligned}. \tag{4}$$

Obviously, $\mathbf{E}_{0+}(x)$ and $\mathbf{E}_{0-}(x)$ are the two orthogonal eigenwaves with the effective indices $n_\pm = n_0 \pm \kappa_0$ related to linear and magnetically induced circular birefringence. Thus, according to Eq. (3), Eq. (1) can also be rewritten as

$$\begin{aligned} \mathbf{E}(x,y,z,t) = \frac{1}{2}\mathbf{F}(y,z)\big[&\hat{\mathbf{e}}_+\mathbf{E}_{0+}(0)\exp(\mathrm{j}\kappa x) \\ &+ \hat{\mathbf{e}}_-\mathbf{E}_{0-}(0)\exp(-\mathrm{j}\kappa x)\big]\mathrm{e}^{\mathrm{j}(\omega t - \beta_0 x)} + c.c., \end{aligned} \tag{5}$$

where $\beta_0 = n_0 k_0$, and $\mathbf{E}_{0+}(0)$ and $\mathbf{E}_{0-}(0)$ are the incident optical fields at $x = 0$. From Eq. (5), the propagation constants of the elliptical eigenwaves can be expressed as $\beta_\pm = \beta_0 \pm \kappa$ and are dependent on the SOPs along with the magnetization direction. The polarization states of the elliptical eigenwaves $\mathbf{P}_\pm$ can be expressed by the following Jones matrix forms:

$$\mathbf{P}_+ = \frac{1}{\sqrt{1+\eta^2}}\begin{pmatrix} 1 \\ \mathrm{j}\eta \end{pmatrix}, \mathbf{P}_- = \frac{1}{\sqrt{1+\eta^2}}\begin{pmatrix} \eta \\ -\mathrm{j} \end{pmatrix}. \tag{6}$$

Subsequently, a linear birefringent MFBG may be regarded as the linear birefringent MO fiber perturbed by the refractive index modulation of FBGs. According to the same coupled-mode analysis used in Ref. [14], the isotropic index grating perturbation does not change the polarization states of the eigen-modes (also called the eigenwaves of MFBGs), just as in the linear birefringent fiber; however, it has a great influence on the amplitude distribution. In general, the polarization states of both eigenwaves are orthogonal to each other and remain fixed inside the MFBGs. The ellipticity of the eigen SOPs depends on the relative magnitude of the linear and magnetically induced circular birefringence. For the uniform index grating $\Delta n(x) = 2\Delta n_g \cos(2\pi x/\Lambda)$, where $2\Delta n_g$ is the amplitude of index variation over a grating period Λ, the transmission and reflection coefficients of the two elliptical eigenwaves in the linear birefringent MFBGs ($t_\pm$ and $r_\pm$) can be expressed by

$$\begin{cases} t_\pm = \dfrac{E_\pm^{\mathrm{f}}(L)}{E_\pm^{\mathrm{f}}(0)} = \dfrac{q_\pm}{q_\pm\cos q_\pm L + \mathrm{j}\delta_\pm \sin q_\pm L} \\ r_\pm = \dfrac{E_\pm^{\mathrm{b}}(0)}{E_\pm^{\mathrm{f}}(0)} = \dfrac{-\mathrm{j}\kappa_g \sin(q_\pm L)}{q_\pm\cos(q_\pm L) + \mathrm{j}\delta_\pm \sin(q_\pm L)} \end{cases}, \tag{7}$$

where L is the length of the uniform MFBG, the subscript "$\pm$" corresponds to the two orthogonal eigenwaves, and the superscripts "f" and "b" indicate the forward and backward GOWs, respectively. In addition, $\delta_\pm = \beta_\pm(\omega) - \beta_B = n_\pm k_0 - \pi/\Lambda = (\omega - \omega_B)n_\pm/c$, $\beta_B = \pi/\Lambda$, $\omega_B = \beta_B c/n_\pm$, $n_\pm = n_0 \pm \kappa/k_0$, $q_\pm = \sqrt{\delta_\pm^2 - \kappa_g^2}$, and $\kappa_g = k_0 \Delta n_g > 0$. Equation (7) expresses the relation between the birefringent effects and the grating coupling in terms of the parameters κ and κ_g for the first time, regardless of having a form, which is similar to the case of conventional non-magnetic FBGs. From Eq. (7), the PDL of the MFBGs may easily be calculated as well.

In the coupled-mode, the contributions of the Faraday MO effect and grating index are regarded as a whole and added simultaneously into a linear birefringent fiber model, similar to the procedure used in Ref. [12]. In the slowly varying envelope approximation, the coupled-mode equations are of the matrix form given by

$$\frac{\partial}{\partial x}\begin{bmatrix} A_y^{\mathrm{f}}(x) \\ A_z^{\mathrm{f}}(x) \\ A_y^{\mathrm{b}}(x) \\ A_z^{\mathrm{b}}(x) \end{bmatrix} = \begin{bmatrix} -\mathrm{j}(\beta_0 - \beta_B) & -\kappa_{\mathrm{m}}\mathrm{e}^{\mathrm{j}\Delta\beta x} & -\mathrm{j}\kappa_{\mathrm{g}}\mathrm{e}^{\mathrm{j}\Delta\beta x} & 0 \\ \kappa_{\mathrm{m}}e^{-\mathrm{j}\Delta\beta x} & -\mathrm{j}(\beta_0 - \beta_B) & 0 & -\mathrm{j}\kappa_{\mathrm{g}}\mathrm{e}^{-\mathrm{j}\Delta\beta x} \\ \mathrm{j}\kappa_{\mathrm{g}}\mathrm{e}^{-\mathrm{j}\Delta\beta x} & 0 & \mathrm{j}(\beta_0 - \beta_B) & \kappa_{\mathrm{m}}\mathrm{e}^{-\mathrm{j}\Delta\beta x} \\ 0 & \mathrm{j}\kappa_{\mathrm{g}}\mathrm{e}^{\mathrm{j}\Delta\beta x} & -\kappa_m e^{\mathrm{j}\Delta\beta x} & \mathrm{j}(\beta_0 - \beta_B) \end{bmatrix}\begin{bmatrix} A_y^{\mathrm{f}}(x) \\ A_z^{\mathrm{f}}(x) \\ A_y^{\mathrm{b}}(x) \\ A_z^{\mathrm{b}}(x) \end{bmatrix}. \tag{8}$$

In general, Eq. (8) can be solved by employing the numerical method, after which the optical field distribution inside the linearly birefringent MFBGs and information on the eigen polarization states can be obtained.

The PDL can be derived from the transmittivities of the eigenwaves. PDL is defined as the maximum polarization sensitivity of a device over all possible input polarization states and is expressed as

$$\mathrm{PDL}(\lambda) = 10 \lg \frac{T_{\max}(\lambda)}{T_{\min}(\lambda)}, \tag{9}$$

where $T_{\max}$ and $T_{\min}$ denote the maximal and minimal power transmittivities through the device, respectively. To determine $T_{\max}$ and $T_{\min}$, we introduce a function $Q[\lambda;(\eta,\theta)] = 10\left|\lg \frac{T[\lambda;(\eta,\theta)]}{T[\lambda;(\eta^*,\theta^*)]}\right|$, where T is the power transmittivity corresponding to each of the two orthogonal input SOPs, namely, (η,θ) and (η^*,θ^*). Our calculation also shows that the equal peak values appear just at the eigen SOPs. Thus, the PDL of the MFBGs can be calculated from

$$\mathrm{PDL}(\lambda) = \max\{Q[\lambda;(\eta,\theta)]\} = \left|10 \lg \frac{T_+(\lambda)}{T_-(\lambda)}\right|, \tag{10}$$

where $T_\pm(\lambda) = |t_\pm(\lambda)|^2$ are the power transmission spectra for the two orthogonal eigenwaves. Equation (10) has also been validated according to the principle of PDL measurement based on the Mueller matrix method[15], in which $T_{\max} = m_{11} + \sqrt{m_{12}^2 + m_{13}^2 + m_{14}^2}$, $T_{\min} = m_{11} - \sqrt{m_{12}^2 + m_{13}^2 + m_{14}^2}$, and $m_{1k}(k = 1,2,3,4)$ are the elements of the Mueller matrix and can be derived from Eqs. (6) and (7) by the coordinate transformation.

In the birefringent FBGs in the absence of the Faraday effect, $\kappa_{\mathrm{m}} = 0$ and $\mathbf{M}(x)$ is diagonal because $\sin\tau = 0$, $\cos\tau = 1$, and $\kappa = \kappa_{\mathrm{b}}$, indicating that the y and z axes are the so-called eigen coordinate axes. In this case, Eq. (7) is reduced to the same results as given in Ref. [15]. The resulting PDL spectral curve has two symmetric peaks, and both of the peak PDL and the corresponding wavelength separation depend on the magnitude of linear birefringence (Fig. 1). The peak PDL may also be used to measure the linear birefringence of the FBGs only in the range of low linear birefringence ($\Delta n_{\mathrm{b}} \le 5 \times 10^{-5}$ for our calculation). In the case of a larger linear birefringence, one can resort to the change of wavelength spacing between the PDL peaks.

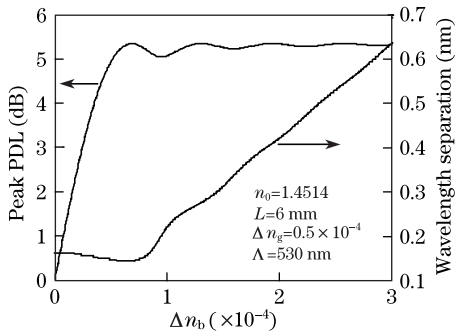

Fig. 1. Variations of the peak PDL and wavelength separation with linear birefringence.

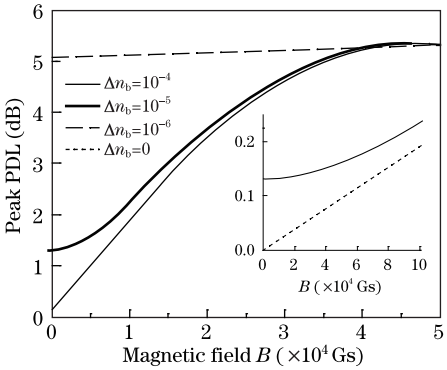

Fig. 2. Dependencies of peak PDL on magnetic field.

In a similar manner, for the linear birefringent MFBGs, the magnetic field dependency of PDL spectra can also be obtained from Eqs. (7) and (10) (Fig. 2). However, the applied magnetic fields hardly lead to the change of the wavelength separation between two symmetric PDL peaks because of the low Verdet constant $V_{\mathrm{B}} = 1.59 \times 10^{-33}\nu^2$ rad/(Gs·m) for the silica fibers, in which ν is the optical frequency in hertz[16]. The peak PDL increases with the linear birefringence inside the MFBG, resulting in the lower limit of linearly measurable magnetic field and magnetic field sensitivity of the peak PDL (Fig. 2). The linear dynamic range of the peak PDL-based magnetic field measurement is dependent on the relative magnitude of linear and magnetically induced circular birefringence. The YIG-based MFBGs and one-dimensional magneto-photonic crystals[17] both have the potential to be used in the magnetic field measurement with high sensitivity.

The theoretical model of linearly birefringent MFBGs presented here can also be used to explain qualitatively the effect of linear birefringence on the PDL of the MFBG in the experiments. Peng *et al.* have measured the peak PDL of fiber grating under the applied magnetic field and attributed the difference of experimental and simulated results to the inherent PDL of FBG[11]. Based on the same parameters used in the experiment (central wavelength $\lambda_0 = 1547.54$ nm, $\Lambda = 535$ nm, $\Delta n_g = 1 \times 10^{-4}$, and $V_{\mathrm{B}} = 8 \times 10^{-5}$ rad/(Gs · m)), we present our calculation results in Fig. 3. The peak PDL increased with Δn_{b} and is similar to the result in Fig. 1. The curve with $\Delta n_{\mathrm{b}} = 2.55 \times 10^{-7}$ is very close to the experimental data for higher magnetic fields, but there is a small discrepancy in the range of small magnetic fields $B < 900$ Gs corresponding to $\Delta n_{\mathrm{m}} < 2{\times}10^{-8}$, which is one order of magnitude smaller than linear birefringence.

To demonstrate further the validity of the theoretical model of the MFBG, we conducted an investigation into the influence of linear birefringence on the magnetic field sensitivity of the uniform MFBG with a fiber-type polarization controller (FPC). To a great extent, the FPC acted as a compensator for the external fiber linear birefringence. At the same time, the FPC was used to adjust the linear birefringence outside the MFBG and the corresponding PDL was measured separately to be 0.206 dB. In theory, the total PDL was calculated from the Jones matrices of the MFBG and FPC, in which the rotation angle between their birefringence axes were also taken into account. Our experimental and theoretical results are illustrated in Fig. 4. The parameters of the

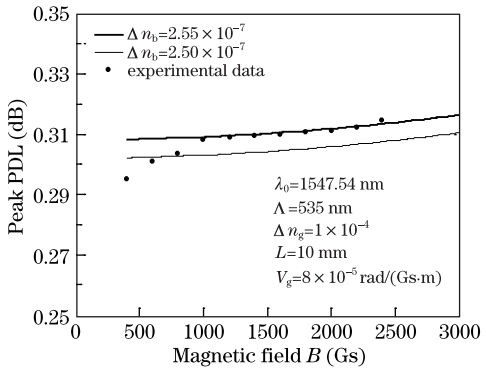

Fig. 3. Comparison of our theoretical results and experimental data in Ref. [11].

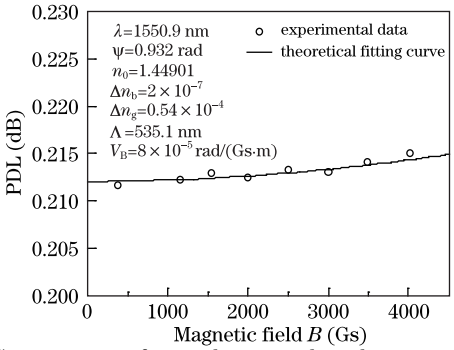

Fig. 4. Comparison of our theoretical and experimental results.

MFBG used in the experiment are labeled in the figure. The wavelength of the optical source was $\lambda = 1550.9$ nm. Given that the fitted theoretical curve corresponds to the rotation angle $\psi = 0.932$ rad and $\Delta n_{\rm b} = 2 \times 10^{-7}$, it is clear that the theoretical model may be used to fit the experimental data well. A systematic investigation will be described in a future article. Meanwhile, the pilot study has shown that the linear birefringence inside the MFBG cannot be compensated completely by adjusting the FPC, although the inherent PDL has been eliminated in the absence of magnetic field. The control of the interior linear birefringence is the crucial factor that must be considered in the improvement of the magnetic field sensitivity of the MFBG. At the same time, the PDL contribution of the exterior devices should be as small as possible.

In conclusion, according to the coupled-mode perturbation theory, the interaction between the Faraday effect and the grating Bragg diffraction in linear birefringent MFBGs is investigated analytically and numerically using the eigen-mode and coupled-mode approaches, respectively. The first method gives expression to the transmittivity of the eigen SOPs, which is useful for the derivation of the PDL spectrum. The magnetic-field dependency of the peak PDL and influence of intrinsic linear birefringence have also been analyzed. Both the magnetic-field sensitivity and linearly dynamic range of peak PDL have been shown to reduce with the increase of linear birefringence. The MFBG with small linear birefringence has also been applied to the peak PDL-based magnetic-field measurement. By comparison, the second method is more efficient for analyzing the SOP evolution inside the MFBG. Finally, we utilize the theoretical model of the MFBG to explain the available experimental data.

This work was supported by the National "863" Program of China (No. 2009AA01Z216) and the Program for New Century Excellent Talents in University (NCET).

References

1. L. Pei, R. Zhao, T. Ning, X. Dong, Y. Wei, C. Qi, and Y. Ruan, Acta Opt. Sin. (in Chinese) **29,** 308 (2009).
2. L. Lu, J. Zheng, Y. Wei, P. Chen, T. Pu, and Y. Li, Chinese J. Lasers (in Chinese) **36,** 2939 (2009).
3. W. Ren, P. Tao, Z. Tan, Y. Liu, and S. Jian, Chin. Opt. Lett. **7,** 775 (2009).
4. T. Mao, J. Chen, and C. Hu, J. Cryst. Growth **296,** 110 (2006).
5. A. Maeda and M. Susaki, IEEE Trans. Magn. **42,** 3096 (2006).
6. B. Wu, X. Lu, and K. Qiu, Chin. Phys. Lett. **27,** 067803 (2010).
7. A. D. Kersey and M. J. Marrone, Proc. SPIE **2360,** 53 (1994).
8. J. L. Arce-Diego, R. López-Ruisánchez, J. M. López-Higuera, and M. A. Muriel, Opt. Lett. **22,** 603 (1997).
9. J. L. Cruz, M. V. Andres, and M. A. Hernandez, Appl. Opt. **35,** 922 (1996).
10. S. T. Oh, W. T. Han, U. C. Paek, and Y. Chung, Opt. Express **12,** 724 (2004).
11. H. Peng, Y. Su, and Y. Li, Proc. SPIE **7134,** 71342C (2008).
12. M. Torfeh, L. Courtois, L. Smoczynski, H. le Gall, and J. M. Desvignes, Physica **89B,** 255 (1977).
13. A. Yariv, *Optical Electronics in Modern Communications* (Oxford University Press, New York, 1997).
14. B. Wu, X. Liu, and K. Qiu, Opt. Fiber Technol. **15,** 165 (2009).
15. S. Bette, C. Caucheteur, M. Wuilpart, and P. Mégret, Opt. Commun. **269,** 331 (2007).
16. J. Noda, T. Hosaka, Y. Sasaki, and R. Ulrich, Electron. Lett. **20,** 906 (1984).
17. M. Vasiliev, K. E. Alameh, V. I. Belotelov, V. A. Kotov, and A. K. Zvezdin, J. Lightwave Technol. **24,** 2156 (2006).